Topology optimization for coated structures

Anders Clausen[1], Erik Andreassen[2], Ole Sigmund[3]

Technical University of Denmark, Lyngby, Denmark
[1] andcla@mek.dtu.dk
[2] erand@mek.dtu.dk
[3] sigmund@mek.dtu.dk

1. Abstract
This paper presents new results within the design of three-dimensional (3D) coated structures using topology optimization. The work is an extension of a recently published two-dimensional (2D) method for including coated structures into the minimum compliance topology optimization problem. The high level of control over key parameters demonstrated for the 2D model can likewise be achieved in 3D. The effectiveness of the approach is demonstrated with numerical examples, which for the 3D problems have been solved using a parallel topology optimization implementation based on the PETSc toolkit.
2. Keywords: Topology optimization, Coating, 3D optimization.

3. Introduction

This study considers the design of coated structures in 3D using topology optimization. Metal coating of polymer structures can be used to enhance functional or visual properties. Many polymers are more easily processed into complex shapes than metals. By coating polymer structures with metal it is possible to combine the processing and cost advantages of polymers with the performance benefits of metal.

This work is based on a recently published paper [4], which introduced a novel method for modeling coated structures and material interface problems in relation to density based topology optimization. The original method was limited to 2D applications. In this paper the method is extended to 3D. As in the 2D version, the method assumes perfect bonding between the substrate and the coating material.

The paper considers minimum compliance problems. The approach is applicable for density based topology optimization and draws on the basic ideas of the SIMP approach (see e.g. [3]). As described in detail in the paper on 2D coating [4], the usual stiffness interpolation from SIMP is extended to include spatial gradients of the filtered design field. This allows to identify material interfaces and enforce coating. In order to control the spatial gradient field, and thereby assure a uniform coating thickness, a two-step filtering approach is applied.

The ability to accurately describe material interfaces is often mentioned as an advantage of level-set based approaches, for which interfaces are implicitly defined by iso-contours of a level-set function (for a review of level-set based topology optimization, see e.g. [9]). An example is [10], where a level-set based method for including material interface properties in the optimization of multi-phase elastic and thermoelastic structures is introduced. The method introduced in [4], and extended in this paper, shows that it is also possible to accurately capture material interfaces using a density based approach.

4. Problem formulation

This section recapitulates the optimization problem as defined in [4] with focus on conveying the main ideas of the approach. Furthermore, the relevant parameters chosen for the present study are described. The material model and characteristic properties are reported in the continuous versions of the design field and filters. Only when defining the optimization problem, the discretized version is introduced.

A coated structure is characterized by a base structure made of one material (referred to as the substrate in a process context) and a coating made of a different material. Initially, no limitations are put on the shape and dimensions of the base structure, whereas the coating is assumed to have a constant, predefined thickness, t_{ref}, at all surfaces of the base structure. Fig. 1 shows a sketch of a 3D coated structure. It is important to notice that the prescribed coating thickness, t_{ref}, is a fixed parameter which is defined as part of the design problem. For the optimization problem, it is convenient to define the coating based on the spatial gradient of the design field in order to assure sufficient design freedom. The modeled coating may be characterized by a thickness, t, which depends on the design field. This approach assures sufficient design freedom, but must be combined with a method to control the gradient field in order to end up with a design where $t = t_{\text{ref}}$.

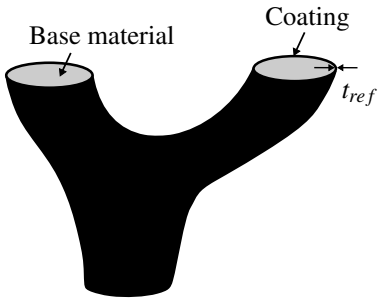

Figure 1: Illustrative sketch of a 3D coated structure with coating thickness t_{ref}.

To control the shape of the gradient a two-step filtering process is applied. First, the design field, μ, is smoothed (giving $\hat{\mu}$) and projected (giving $\varphi = \bar{\hat{\mu}}$). This projection defines the base structure.

In order to identify the interface of the base structure, a second smoothing is applied (giving $\hat{\varphi}$). The norm of the spatial gradient, $\|\nabla\hat{\varphi}\|_\alpha$, in this second smoothed field is used to identify the interface (the index α means that the norm is normalized, such that its maximum value is one - see details in Section 4.4). The normalized norm is subsequently projected to model a sharp interface. This field, which is denoted $\overline{\|\nabla\hat{\varphi}\|_\alpha}$, defines the coating.

Thus, the desired coating thickness is defined indirectly by setting the filter radius used for the second smoothing (R_2), as this filter determines the width of the interface region.

4.1. Filters

In order to regularize the optimization problem a smoothing is performed using a so-called PDE-filter [6] with appropriate boundary conditions. The first smoothing (from μ to $\hat{\mu}$) is performed by solving the equation:

$$-\Big(\frac{R_1}{2\sqrt{3}}\Big)^2\nabla^2\hat{\mu} + \hat{\mu} = \mu \tag{1}$$

where the spatial neighborhood is defined by the magnitude of the scalar in front of the Laplacian. In the above form, R_1 corresponds to the filter radius in standard filtering techniques. Furthermore, a projection method ([5], [7]), in the form first proposed in [11], is applied as a means of obtaining black-and-white designs. The projection is determined by the step "sharpness" β and the threshold parameter $\eta \in [0;1]$.

4.2. Interpolation function

The coating material has the mass density ρ^0 and elasticity modulus E^0. The material properties of the base material are defined as ratios of the coating material's properties. The mass density ratio is $\lambda_m \in]0,1[$ and the stiffness ratio is $\lambda_E \in]0,1[$. For simplicity, both materials are assumed to be isotropic with a Poisson's ratio, ν^0, independent of interpolation density.

The physical density, ρ, and stiffness, E, are defined as interpolations of φ and $\overline{\|\nabla\hat{\varphi}\|_\alpha}$:

$$\rho(\varphi, \overline{\|\nabla\hat{\varphi}\|_\alpha}) = \rho^0\left[\lambda_m\varphi + (1-\lambda_m\varphi)\overline{\|\nabla\hat{\varphi}\|_\alpha}\right] \tag{2}$$

$$E(\varphi, \overline{\|\nabla\hat{\varphi}\|_\alpha}) = E^0\left[\lambda_E\varphi^p + (1-\lambda_E\varphi^p)(\overline{\|\nabla\hat{\varphi}\|_\alpha})^{p_g}\right] \tag{3}$$

Opposite to the original paper [4] a distinction is made between the penalization parameters, p and p_g, penalizing φ and $\overline{\|\nabla\hat{\varphi}\|_\alpha}$, respectively.

Note that when the normalized gradient norm approaches its maximum value ($\overline{\|\nabla\hat{\varphi}\|_\alpha} = 1$), i.e. at the interface region, the physical density and stiffness approach ρ^0 and E^0, respectively:

$$\begin{aligned}\rho_{coating}(\varphi,1) &= \rho^0\left[\lambda_m\varphi + (1-\lambda_m\varphi)\right] = \rho^0\\ E_{coating}(\varphi,1) &= E^0\left[\lambda_E\varphi^p + (1-\lambda_E\varphi^p)\right] = E^0\end{aligned} \tag{4}$$

Opposite, when the gradient norm approaches zero, i.e. when going away from the interface, the second term in Equation (2) and (3) vanishes. In these regions $\varphi = 1$ corresponds to base structure, whereas $\varphi = 0$ corresponds to void.

4.3. Optimization problem

The optimization problem is a standard minimum compliance problem with a constraint on the volume. For the discretized problem the continuous fields are replaced with vectors of element values (e.g. $\boldsymbol{\mu}$ instead of μ).

The global stiffness matrix, $\mathbf{K}$, is defined as:

$$\mathbf{K}(\boldsymbol{\mu}) = \sum_e \mathbf{k}_e(\boldsymbol{\mu}) = \sum_e E_e(\varphi_e(\boldsymbol{\mu}), \overline{\|\nabla\hat{\varphi}_e(\boldsymbol{\mu})\|}_\alpha)\mathbf{k}_e^0 \tag{5}$$

where $\mathbf{k}_e$ is the element stiffness matrix, and $\mathbf{k}_e^0$ is the element stiffness matrix for an element with unit elasticity modulus. To avoid a singular system in the numerical interpolation, the first term in Eq. (3), $\lambda_E\varphi_e^p$, is replaced with $\lambda_{E,\min} + (\lambda_E - \lambda_{E,\min})\varphi_e^p$.

The optimization problem is defined in the following way:

$$\begin{aligned} \min_{\boldsymbol{\mu}}: \quad & c(\boldsymbol{\mu}) = \mathbf{U}^\mathbf{T}\mathbf{K}\mathbf{U} \\ \text{subject to:} \quad & \mathbf{K}\mathbf{U} = \mathbf{F} \\ & g(\boldsymbol{\mu}) = V(\boldsymbol{\mu})/V^* - 1 \leq 0 \\ & 0 \leq \mu_e \leq 1, \quad \forall e \end{aligned} \tag{6}$$

Here c is the compliance, $\mathbf{U}$ and $\mathbf{F}$ are the global displacement and force vectors, respectively, g is the volume constraint, $V(\boldsymbol{\rho}(\boldsymbol{\mu})) = \sum v_i\rho_i(\boldsymbol{\mu})$ is the material volume and V^* is the maximum allowed volume.

Design updates are performed based on sensitivities using MMA ([8]). The sensitivity analysis is performed in a way analogous to the 2D version.

4.4. Parameters

In the second smoothing step, where the filter radius is set to R_2, the filter radius is computed based on the specified coating thickness t_{ref} as $R_2 = 2.5t_{\text{ref}}$. This is independent on whether a 2D or 3D problem is considered. The same holds for the normalization factor α, which is defined as the inverse of the maximum possible gradient norm of the second smoothed field, $\hat{\varphi}$. It takes the value $\alpha = R_2/\sqrt{3}$.

As opposed to [4], the penalization factor on the gradient part is distinguished from the penalization on the design variable. This is done because in 3D it is usual to work with lower volume fractions. Thus, if the gradient field were to be penalized in the initial phase of the optimization, the corresponding sensitivities would be small. This can be circumvented by instead introducing the penalization on the gradient field gradually.

A continuation scheme is adopted for both the penalization parameters and the projection. The penalization for $\overline{\|\nabla\hat{\varphi}\|}_\alpha$ is initialized as $p_g = 1$ and gradually increased to $p_{g,max} = 3$. When $p_{g,max}$ is achieved the penalization for φ is gradually increased from $p = 3$ to $p_{max} = 4$. The two projections are performed with identical parameters. The threshold is $\eta = \eta_g = 0.5$. The sharpness parameter is initialized with $\beta = 16$. After reaching p_{max}, β is gradually increased to 64 by doubling at convergence (or after 100 iterations since last update).

The parallel 3D implementation is based on the topology optimization framework [1] utilizing PETSc [2]. This allows solving problems with millions of design elements, which is necessary in order to have a fine enough discretization to capture the coating.

5. Results

The approach is demonstrated by solving the optimization problem in Eq. (6) on both a 2D domain and an equivalent 3D domain. The design problem for both cases consists of a distributed load applied at the entire top surface. The 2D domain is illustrated in Fig. 2. The full domain has the dimensions 200 by 50, however, by using a symmetry condition at the right edge only half of the domain is modeled. The center half of the bottom layer is clamped. The domain is discretized using bi-linear elements with two elements per unit length. The total load equals 10. The coating thickness is set to $t_{ref} = 1$.

The 3D design problem is similar to the 2D problem. Denote the vertical direction by z and the two horizontal directions by x and y. Again, a distributed load is applied at the entire top surface ($z = z_{max}$). The load sums up to 0.25. The central area of the bottom layer ($z = 0$) is clamped. The *central area* here refers to points which are simultaneously in the central half in the x and y directions (see the optimized structure in Fig. 4 for visualization). Only a quarter of the domain is modeled, using symmetry constraints in both the x and y directions.

When discretizing the 3D problem the chosen domain decomposition approach from the parallelized PETSc code has to be taken into account. Using four decompositions, the number of elements in each direction should be a multiple of 16 (2^4). Simultaneously it is chosen to let the coating thickness $t_{ref} = 1$ correspond to an integer number of elements. This is not a requirement, but makes it easier to visually assess the results. Bearing these two choices in mind the full domain dimensions are defined as $192 \times 96 \times 48$ (a 4:2:1 length ratio), such that a

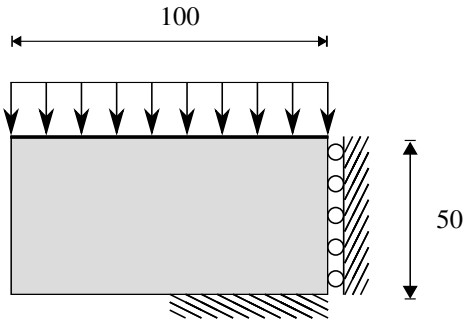

Figure 2: Design domain for the 2D problem, using a symmetry condition at the right edge.

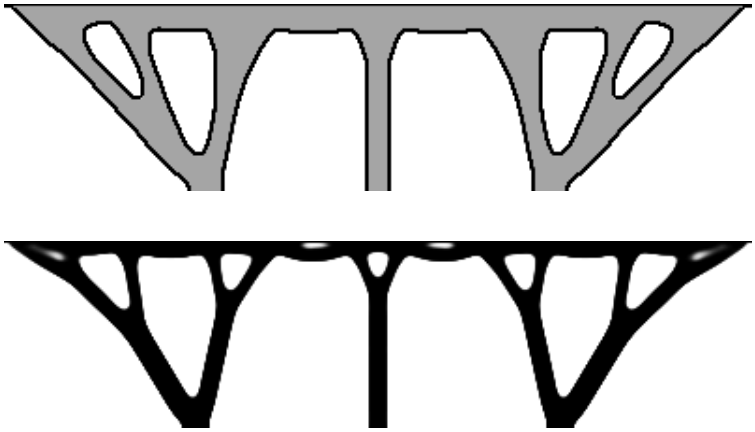

Figure 3: Optimized results in 2D. Top: Coated structure ($c = 814.9$). Bottom: Solid structure ($c = 636.0$).

quarter domain has the dimensions $96 \times 48 \times 48$ and can be resolved with $288 \times 144 \times 144$ tri-linear elements. This slight modification of dimensions compared to the modeled 2D domain (100×50) is justified by the easier interpretation of the results.

For both problems the material parameters of the coating and solid material are $\rho^0 = 1$ and $E^0 = 1$. The base material is defined by $\lambda_E = 0.35$ and $\lambda_m = 0.6$. The first filter radius is $R_1 = 10$. The elements in the topmost layer (at the loaded surface) are set as passive, solid elements. The boundary conditions for the PDE-filter are chosen as homogeneous Neumann conditions at all edges. For the 3D case, the projection sharpness, β, is initialized as 8 rather than 16 in order to stabilize the optimization.

The optimized results for the 2D problem are shown in Fig. 3 for both a coated structure and a solid structure (corresponding to $\lambda_E = \lambda_m = 1$). In the coated structure, the base material has a constant density and the coating is seen to be applied with a uniform thickness everywhere at the structure. The topology of the coated structure is simpler than for the solid structure, as the low density base material has a lower cost in the volume constraint than the solid material. The compliance for the coated structure is larger than for the solid structure, as the stiffness of the base material is disproportionately low with respect to its weight compared to the solid material.

Figure 4 shows the optimized coated structure for the full 3D problem viewed from below. The coating material is visualized in light blue at 35 % transparency, while the base material is light gray. Note that the clamped part of the bottom surface is clearly traced out by the structure. The coating material is again applied in a highly uniform manner at all visible interfaces.

The coated structure is compared with a solid structure optimized with the same parameters in Fig. 5. Only the modeled quarter part of each structure is shown. The structures are compared in full height and for two cross sections at 75 % and 50 % height. First consider the full height structures (a-b). The two structures show the same trend as their 2D equivalents in Fig. 3. The topology for the coated structure is simpler with a significantly lower number of holes. Again, the compliance for the coated structure is larger than for the solid structure due to the disproportionately low stiffness of the base material.

The cross sections in (c-f) further illustrate that the coating material is applied uniformly over the structure. In

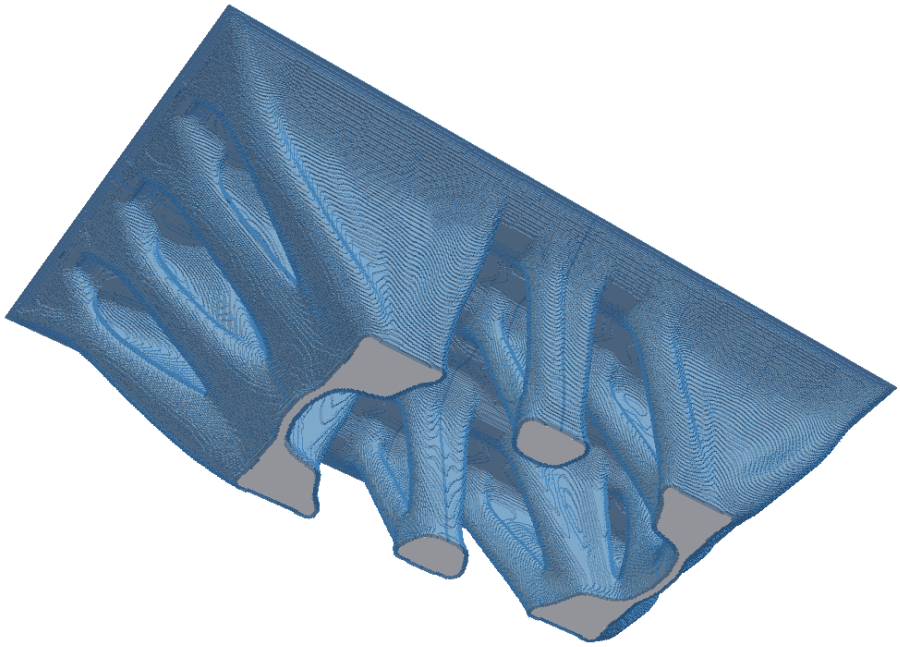

Figure 4: Full 3D structure optimized using the coating approach. The coating material is rendered at 35% transparency to visualize the internal base structure.

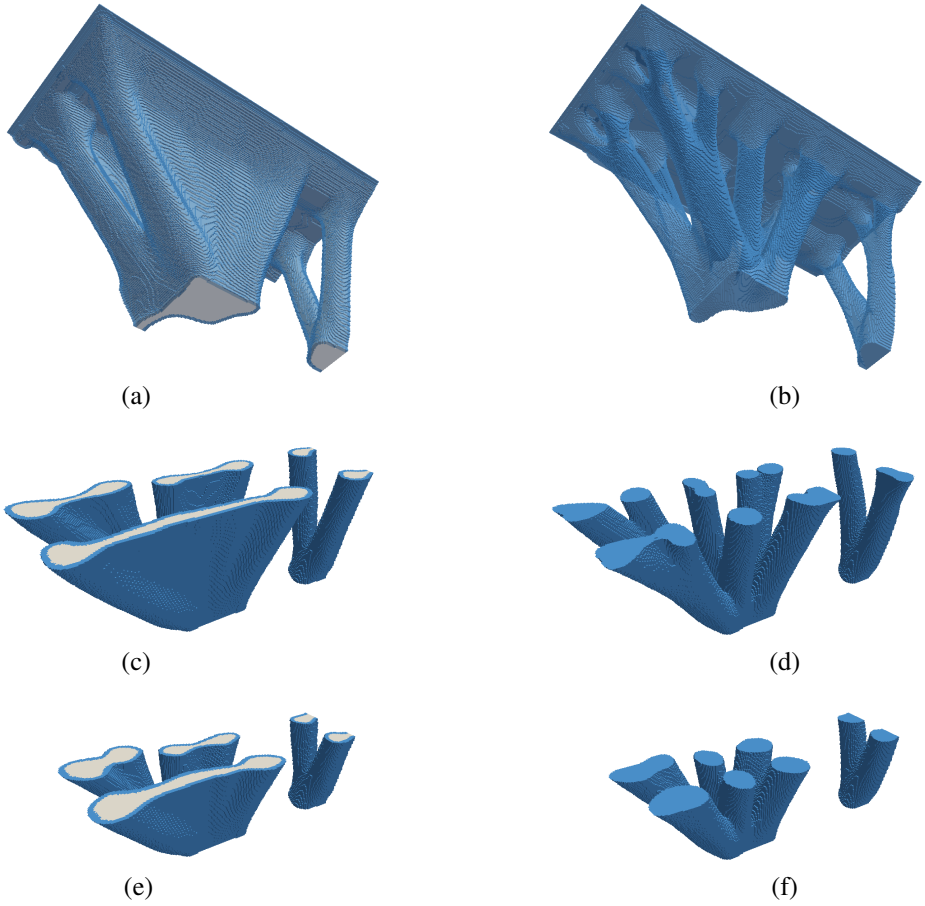

Figure 5: Optimized results in 3D (quarter domain). Left column: Coated structure ($c = 0.2742$). Right column: Solid structure ($c = 0.1420$). (a-b) View from below. Coating and solid material shown at 35% transparency. (c-d) Cross section at 75% height, view from above. (e-f) Cross section at 50% height, view from above.

addition, the figures very clearly show the difference in topology between the coated and solid structures. The pure solid structure continues to branch out in a higher number of members with increasing z-coordinate, whereas the coated structure consists of a few members which do not branch out but rather stay connected while adapting the cross sectional area.

6. Conclusion

It has been shown that coated structures in 3D can be designed using topology optimization. The approach is demonstrated on equivalent design problems in 2D and 3D. The high level of control over the modeled coating which is earlier demonstrated for the 2D model is likewise achieved in 3D.

7. Acknowledgments

The authors acknowledge financial support from the Villum Foundation (the NextTop project) and DTU Mechanical Engineering.

8. References

[1] N. Aage, E. Andreassen, and B. S. Lazarov. Topology optimization using PETSc: An easy-to-use, fully parallel, open source topology optimization framework. *Structural and Multidisciplinary Optimization*, Published online:1–7, 2014.

[2] S. Balay, S. Abhyankar, M. F. Adams, J. Brown, P. Brune, K. Buschelman, V. Eijkhout, W. D. Gropp, D. Kaushik, M. G. Knepley, L. C. McInnes, K. Rupp, B. F. Smith, and H. Zhang. PETSc Web page, 2014.

[3] M. P. Bendsøe and O. Sigmund. *Topology Optimization. Theory, Methods and Applications*. Springer, 2003.

[4] A. Clausen, N. Aage, and O. Sigmund. Topology optimization of coated structures and material interface problems. *Computer Methods in Applied Mechanics and Engineering*, Available online, 2015.

[5] J. Guest, J. Prevost, and T. Belytschko. Achieving minimum length scale in topology optimization using nodal design variables and projection functions. *International Journal for Numerical Methods in Engineering*, 61(2):238–254, 2004.

[6] B. S. Lazarov and O. Sigmund. Filters in topology optimization based on helmholtz-type differential equations. *International Journal for Numerical Methods in Engineering*, 86(6):765–781, 2011.

[7] O. Sigmund. Morphology-based black and white filters for topology optimization. *Structural and Multidisciplinary Optimization*, 33(4-5):401–424, 2007.

[8] K. Svanberg. Method of moving asymptotes - a new method for structural optimization. *International Journal for Numerical Methods in Engineering*, 24(2):359–373, 1987.

[9] N. P. van Dijk, K. Maute, M. Langelaar, and F. Van Keulen. Level-set methods for structural topology optimization: a review. *Structural and Multidisciplinary Optimization*, 48(3):437–472, 2013.

[10] N. Vermaak, G. Michailidis, G. Parry, R. Estevez, G. Allaire, and Y. Bréchet. Material interface effects on the topology optimization of multi-phase structures using a level set method. *Structural and Multidisciplinary Optimization*, Published online:1–22, 2014.

[11] S. Xu, Y. Cai, and G. Cheng. Volume preserving nonlinear density filter based on heaviside functions. *Structural and Multidisciplinary Optimization*, 41(4):495–505, 2010.